

GIS Flood Susceptibility Model Predicts Pond Inundation in a Monsoon Environment

Mason Maurer

1 Introduction

Flooding is considered to be a significant natural hazard that can have serious impacts on ecosystems and human life (Choubin et al., 2018; Talbot et al., 2018). Since flood events are primarily driven by heavy rainfall and/or snowmelt, areas that experience monsoon seasons can be especially susceptible to flooding (Choubin et al., 2018; Talbot et al., 2018).

The North American Monsoon brings a period of intense rainfall to the southwestern United States and northwestern Mexico, starting in July and ending in mid-September (Adams et al., 1997). Rainfall that occurs during this monsoon season can be categorized as having a short duration, high intensity, and spatial variability (Gendreau et al., 2021). The areas affected by the North American Monsoon experience dry periods both prior to and after the rainfall period, with the dry conditions in May and June being particularly extreme (Adams et al., 1997).

The area affected by these monsoons will typically experience rainfall during the winter months as well, especially during years of El Nino, which creates conditions that allow for increased precipitation in areas of the southwestern United States (Goodrich et al., 2008). However, the precipitation that occurs during the winter months is often lower in intensity compared to the thunderstorms that occur during the summer monsoon season (Goodrich et al., 2008). As a result, much of the surface runoff that contributes to stream flow, as well as heavy

rainfall events that contribute to the accumulation of water in desert pond basins, occur during the months of the summer monsoon season (Goodrich et al., 2008).

While it is true that flooding can have devastating effects on things such as agriculture and urban infrastructure, flooding has also been shown to provide several benefits to aquatic ecosystems (Bui et al., 2019; Talbot et al., 2018). The positive impacts of flooding on aquatic ecosystems include recharging groundwater and wetlands, rejuvenating soil fertility, and creating new habitat for wildlife (Talbot et al., 2018). The southwestern United States contains several small ponds that provide a home for aquatic wildlife, some of which were human made for the purpose of providing livestock with water (Gendreau et al., 2021). These ponds, whether they were developed naturally or by humans, now support several different aquatic species (Gendreau et al., 2021).

An important aspect in understanding the stability and diversity of these aquatic ecosystems is hydroperiod, which is the amount of time that a fresh water body holds water (Gendreau et al., 2021). Understanding hydroperiods can help to provide information related to species richness and reproductive success of aquatic amphibian species (Paton et al., 2002; Gendreau et al., 2021). Pond hydroperiods can be affected by flood events in different ways (Murray-Hudson et al., 2014). Flooding can directly affect the inundation of ponds, but the frequency and duration of flood events in particular can also have subtle ecological effects (Murray-Hudson et al., 2014).

In semi-arid environments like the southwestern United States, permanent pond systems tend to be scarce (Nhiwatiwa et al., 2016). The inundation of intermittent pond systems can change within a time frame of as little as two weeks (Gendreau et al., 2021). The absence of permanent aquatic habitats coupled with the temporal variability of the intermittent aquatic

systems emphasizes the importance of being able to understand and predict hydroperiods in a semi-arid region.

In this study, I apply a GIS flood susceptibility model to a region in the southwestern United States that contains a number of intermittent aquatic systems, with the primary goal of determining whether or not areas that are more susceptible to flooding are more likely to house ponds that are in the inundation phase of hydroperiod. The model uses precipitation data and a selection of topographical factors to calculate flood susceptibility for each watershed within the study area. All analysis involved with developing and executing the model was conducted in ArcGIS Pro Version 2.9.0 (Esri Inc. 2021).

2 Methods

2.1 Study Area

The study area consists of 387 ponds located in 43 different HUC-12 watersheds in southern Arizona (USGS and USDA - NRCS, 2022). The study area spans parts of Cochise, Pima, and Santa Cruz counties. The watersheds are located in and around the Coronado National Forest, mainly in the Huachuca Mountains, Canelo Hills, and Santa Rita Mountains (Figure 1). The area's dominant land cover types include shrublands, herbaceous grasslands, and evergreen forests. The area has a semi-arid climate and most of the rainfall it experiences can be attributed to the North American Monsoon (Adams et al., 1997; Gendreau et al., 2021).

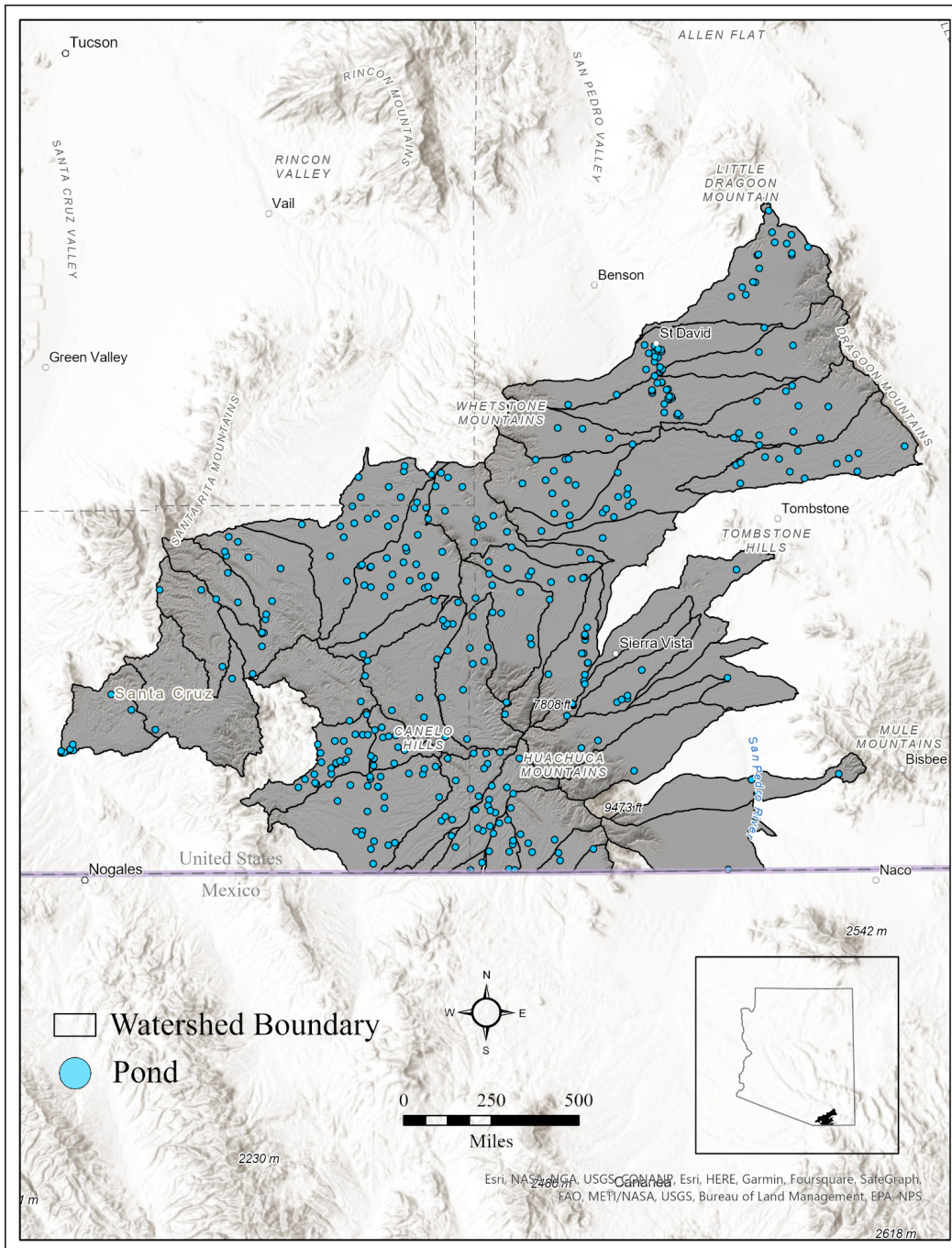


Figure 1: This study is conducted in and around the Coronado National Forest in southeastern Arizona, USA. The boundaries of HUC-12 watersheds are delineated and blue points show the locations of individual ponds that are used in this study, which were identified using Google Earth imagery. Note that some of the watersheds have been cut off at the US/Mexico border. Since none of the ponds used in this study are located in Mexico, the watersheds that extend across the border were clipped to their US area only, for aesthetic purposes.

2.2 Study Dates and Study Ponds

The ponds involved in this study were measured using historical Google Earth imagery. The surface area of each pond was measured each month in which clear satellite imagery was available. Each pond was measured by manually tracing the pond edge using Google Earth's 'Add Polygon' tool, which provided a measure of the pond's surface area (Figure 2a). For the purpose of this study, the measured ponds in each of the study dates were classified as either Wet or Dry, Wet meaning the pond basin had standing water in it and Dry meaning the basin had no standing water in it. The decision to classify ponds this way as opposed to doing so by surface area was based on the fact that there were multiple different issues with some of the satellite imagery that made it difficult to get an accurate measure for the surface area of some ponds.

The most common issues experienced when using satellite imagery to measure ponds were image resolution and the presence of trees that obscured the aerial view of the pond edge. With some of the satellite imagery, while it was clear that the pond contained water, the image was too blurry to provide a clear view of the pond's edges (Figure 2b). Some of the ponds that were measured had their boundaries located beneath tree lines which, when viewed from an aerial perspective, blocked the exact location of the pond edge (Figure 2d). The view of some other ponds was blocked by the shadows created from trees nearby (Figure 2c).

The study dates were chosen based on the months that had satellite imagery available for the most ponds. These months were June 2007, September 2010, April 2013, January 2015, and May 2019.

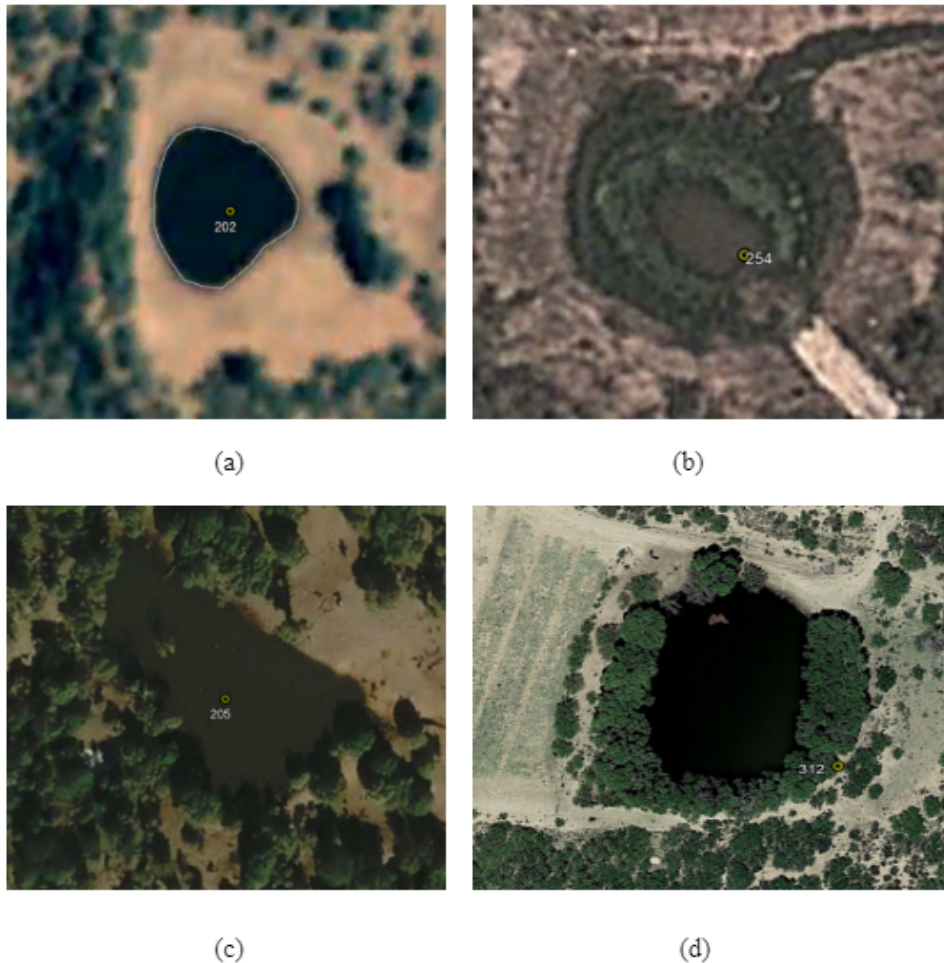


Figure 2: A demonstration of the process and some of the challenges in measuring ponds using Google Earth. (a) shows an unobstructed view of a pond with the polygon edge delineated in white. (b) is an example of an image in which it was difficult to determine where the edge of the standing water in the pond was located. (c) is an image of a pond in which tree shadows obstruct some of the view of the pond edge, making it difficult to accurately measure. (d) is an example of a pond in which tree lines block the edge of the pond.

2.3 Data Variables

I hypothesized that *slope, elevation, distance to streambeds, soil infiltration, and rainfall* would have an influence on flood susceptibility in the study region because these were all variables that were used in previous studies that dealt with flood modeling and were shown to

have an effect on how vulnerable an area is to flooding (Bui et al., 2019; Costache et al., 2019; Choubin et al., 2018; Khosravi et al., 2018).

Slope has been shown to be a very important element that contributes to flooding. Steeper slopes will produce more rapid flows of precipitation runoff compared to low angle slopes (Bui et al., 2019; Khosravi et al., 2018). The presence of steep slopes also decreases infiltration time (Khosravi et al., 2018). The slope layer was created using the ArcGIS Slope tool, with a 30 meter Digital Elevation Model sourced from the United States Department of Agriculture Geospatial Data Gateway as the input raster (USGS, 2022). Slopes in the study area ranged from 0 degrees to 66.63 degrees (Figure 3a).

Elevation is another important factor that influences flooding. Flat, low elevation lands are more likely to flood compared to higher elevations as the lower regions will accumulate the water that flows down from higher regions (Bui et al., 2019; Khosravi et al., 2018). The elevation layer was also created using the 30 meter Digital Elevation Model file (USGS, 2022). Elevations in the study area ranged from 1047 meters to 2877 meters (Figure 3b).

Distance to streambeds has an impact on an area's flood susceptibility, as streams and rivers are the main pathways for flood discharge, which makes the areas adjacent to rivers more prone to flooding (Khosravi et al., 2018; Choubin et al., 2018). The distance to streambeds layer was created using a few different tools. First, the 30 meter DEM was used to create a new layer showing Flow Direction. The Flow Direction tool determines which way water flows out of each cell in the DEM (Figure 4a). The Flow Direction layer was then used to make a Flow Accumulation layer, which shows the total number of pixels that flow into each cell (Figure 4b). From this Flow Accumulation layer, any cell that was found to have an accumulation value greater than 1% of the maximum accumulation value for the entire study area was classified as

being part of a streambed. Finally, by running the Distance Accumulation tool, a layer was created that showed each cell's distance from the nearest streambed. The maximum distance that any cell was from a streambed was 8015.76 meters (Figure 3c).

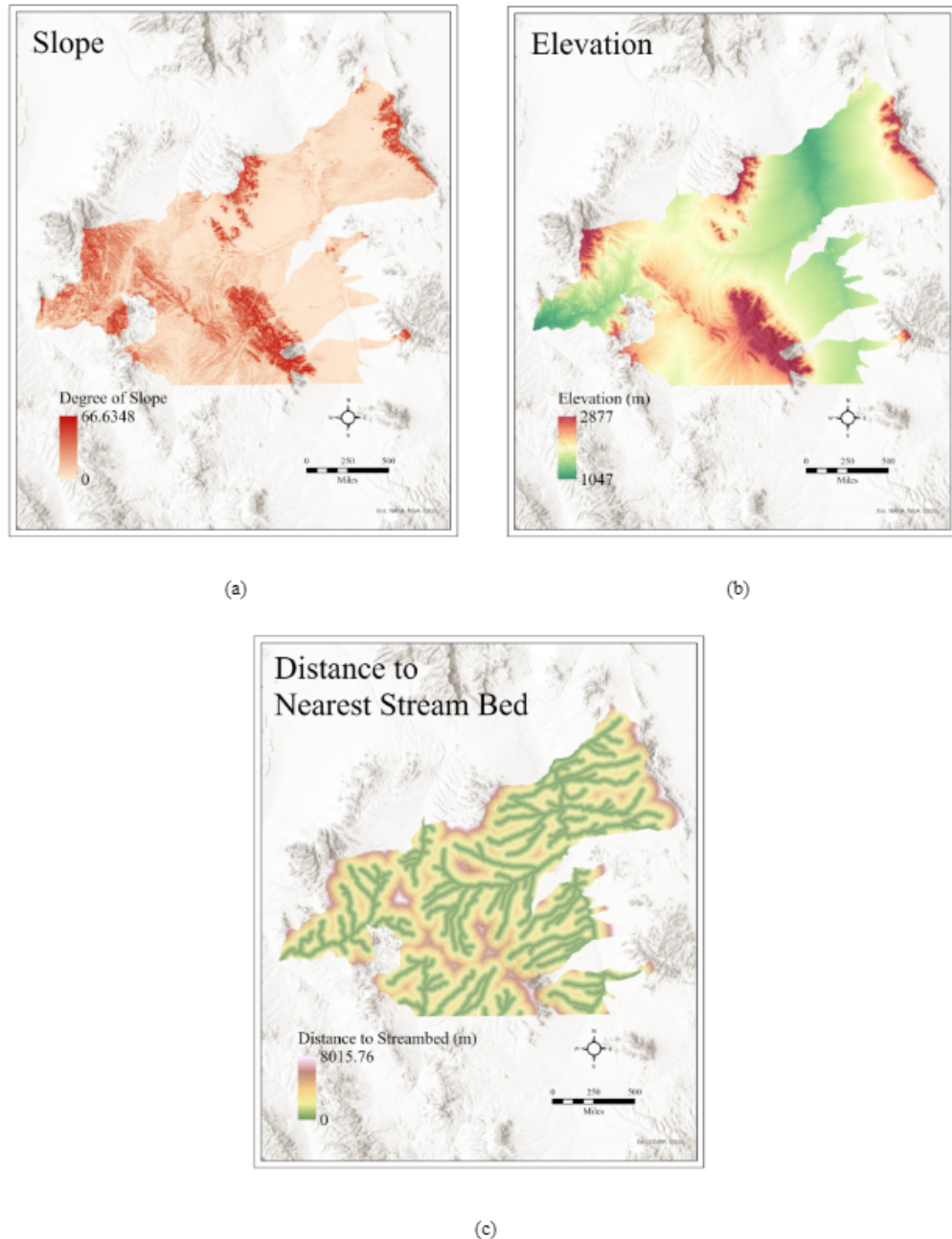


Figure 3: Maps showing the 3 data layers that were created using the 30 Meter Digital Elevation Model. (a) shows the slopes of the study area, with steeper slopes shown in red and flatter areas shown in peach. (b) shows elevation

of the study area, with lower elevations shown in green, moderate elevations shown in yellow, and higher elevations shown in red. (c) shows the distance to the nearest stream bed for each point in the study area, with green areas being the closest to stream beds and red/white areas being the furthest.

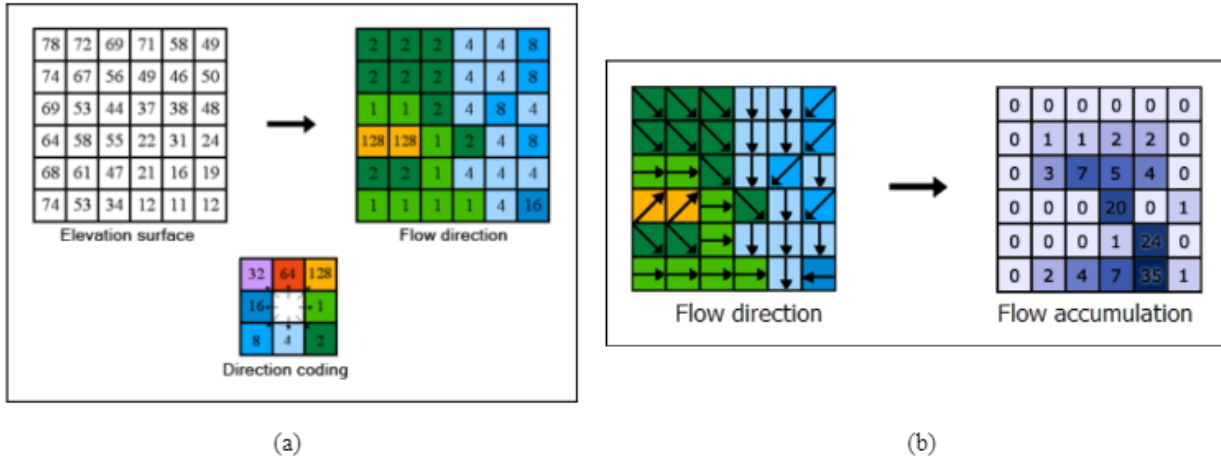


Figure 4: Graphics demonstrating two of the tools used in making the Distance to Nearest Streambed layer. (a) shows how Flow Direction of a raster is calculated, with different outflow directions represented by different numbers. (b) shows how Flow Direction is used to calculate Flow Accumulation, which accumulates the number of cells that flow into each cell.

Soil type and composition will affect how much water can infiltrate the soil (Khosravi et al., 2018). For example, soil that is mostly composed of sand will have a greater infiltration capacity compared to soil that is mostly composed of clay (Basri et al., 2022). The soil layer used in the study was taken from an ESRI produced Soil Survey Map that displays the Soil Survey Geographic Database compiled by the USDA Natural Resources Conservation Service (Esri Inc., 2019). The aspect of the soil data that was used in this study was each soil type's dominant flood condition, which was included in the Soil Survey Map. The study area included parts of three different soil basins: Upper San Pedro, Upper Santa Cruz, and Rilito. Soil layers for the three soil basins were downloaded separately and then combined into a single raster layer in ArcGIS. The

classes of Dominant Flood Condition were ‘Never’, ‘Very Rare’, ‘Rare’, ‘Occasional’, and ‘Frequent’ (Figure 5).

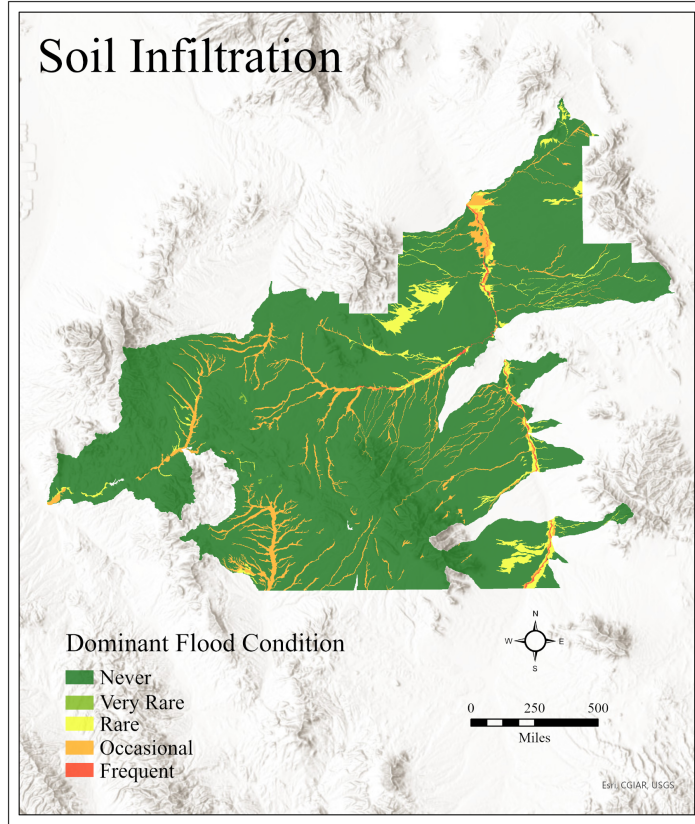


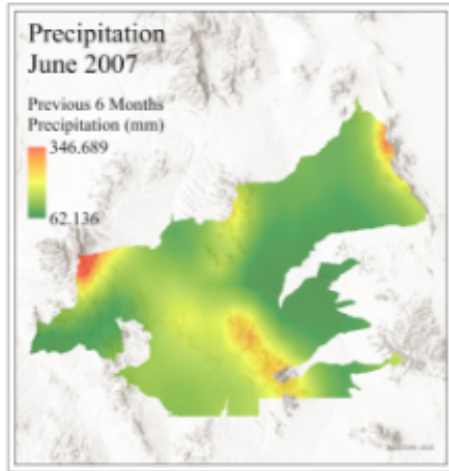
Figure 5: A map showing the dominant flood condition for soils in the study area. Most of the soil has the dominant flood condition of ‘Never’, shown in green. Soils that flood more often are shown in orange and red while soils that rarely flood are shown in yellow and lighter green.

The final variable used in this study was *rainfall*. Rainfall is an important factor of flooding, although the spatial and temporal behavior of rain can make it difficult to effectively incorporate into a flood model (Khosravi et al., 2018). The rainfall data was sourced from the PRISM Climate Group (PRISM, 2014). For this study, the total rainfall from the previous six months was used for each study month (Figures 6a-6e). For example, when running the model for January 2015, the rainfall data for July 2014 through December 2014 was used. Each month’s

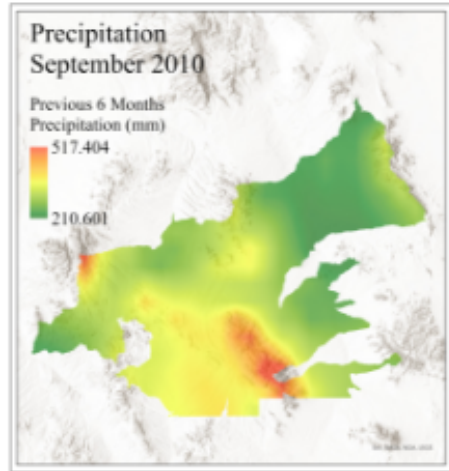
precipitation data was downloaded separately and combined into a single raster file for each study month. Since the PRISM data was only available at a cell resolution of 4 kilometers, each precipitation raster was resampled to a resolution of 30 meters using a Bilinear resampling technique. Bilinear resampling is a method of raster interpolation that uses a weighted distance average of the four nearest input cells to calculate the new value of a cell.

2.4 Data Variable Weighting

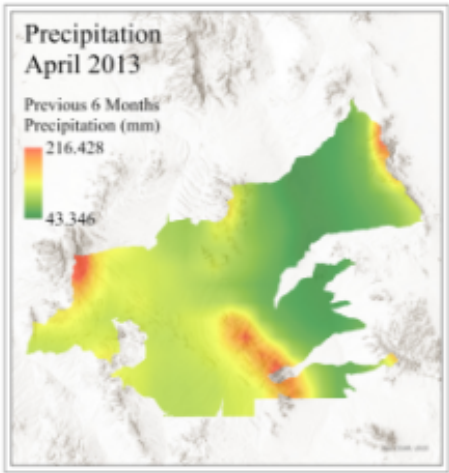
The technique used to model flood susceptibility in this study was a weighted sum model, so the data variables were assigned different weights according to how much influence they have on an area's vulnerability to flooding. In an effort to base the weightings of the variables on science and minimize randomness, I looked at the results of previous research studies that dealt with flood susceptibility and determined an appropriate hierarchy of weights for the different variables based on how much influence they were determined to have on an area's flood susceptibility. According to four previous studies that have been conducted involving flash flood modeling in Iran, Vietnam, and Romania, the most important variable in flood modeling is slope (Bui et al., 2019; Costache et al., 2019; Choubin et al., 2018; Khosravi et al., 2018). Elevation and distance from riversstreams also had notable importance in flood modeling (Bui et al., 2019; Choubin et al., 2018; Khosravi et al., 2018). Rainfall and soil type had a much lower impact on flood susceptibility compared to other variables used in flood modeling (Bui et al., 2019; Choubin et al., 2018; Khosravi et al., 2018). Based on the respective importance of these variables as identified in previous flood modeling studies, the following weights were assigned to each variable: .350 for Slope, .250 for Distance to Streambeds, .200 for Elevation, .125 for Rainfall, and .075 for Soils.



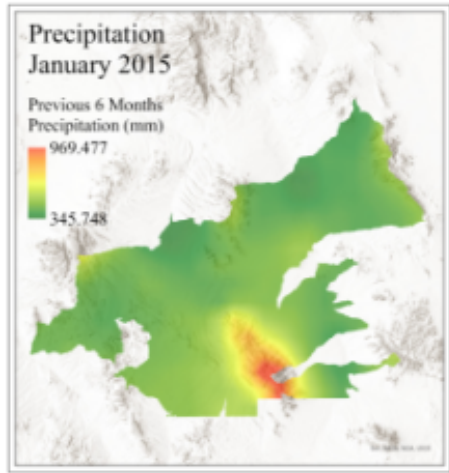
(a)



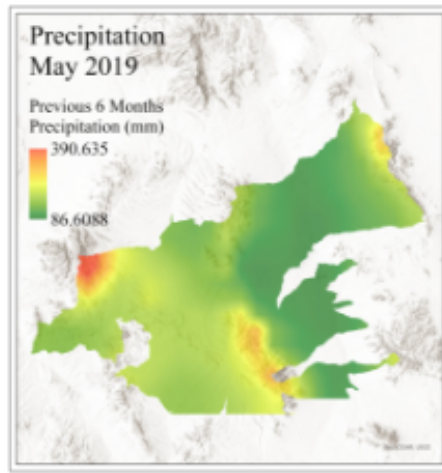
(b)



(c)



(d)



(e)

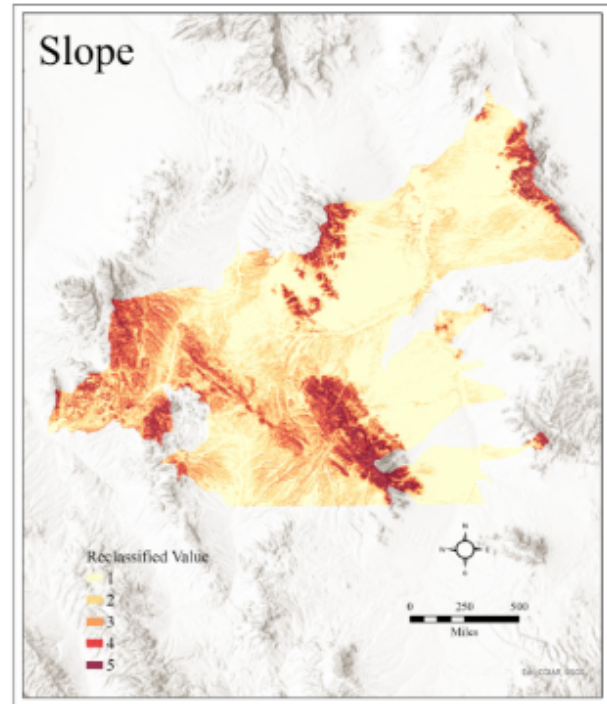
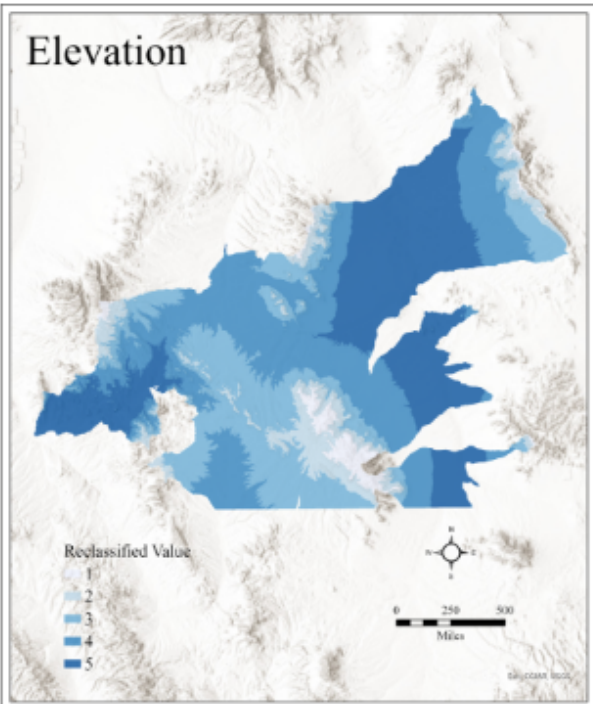
Figure 6: Maps showing the precipitation totals used for each study date: (a) June 2007, (b) September 2010, (c) April 2013, (d) January 2015, (e) May 2019. Areas that received less precipitation are represented in green, while areas that received more precipitation are represented in yellow and orange. The areas that received the most precipitation are represented in red.

2.5 Weighted Sum Model

The flood susceptibility for each study date was calculated using the Weighted Sum tool in ArcGIS. In order to make each data variable compatible with the tool, the raster layers representing the data variables had their values reclassified from 1 to 5. This was done using a Natural Breaks classification method, which assigns values based on natural groupings within the data variables. This classification method was selected because it creates classes in a way that groups similar values together while maximizing the difference between the classes. So, within each data variable layer, the cells that would least contribute to flood susceptibility were assigned a new value of 1 while the cells that would have the largest impact on flood susceptibility were assigned a new value of 5 (Figures 7a-7d, 8a-8e). For example, the steepest slopes, lowest elevations, and areas closest to stream beds were assigned a value of 5.

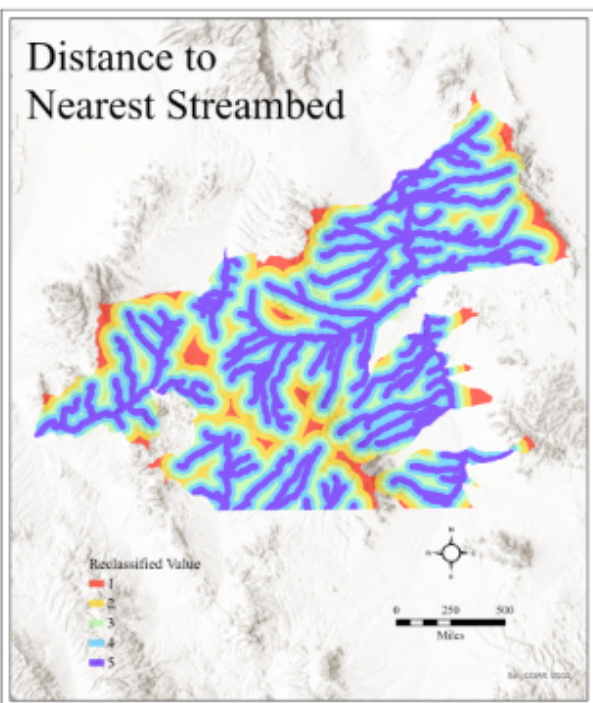
Using the reclassified data variable layers, the Weighted Sum tool was run for each of the five study dates. This created a new raster layer in which each cell was assigned a value that represented that particular cell's susceptibility to flooding. Lower values indicated a lower flood susceptibility and higher values indicated a higher susceptibility.

The HUC 12 watersheds layer was then used to calculate the mean cell value within each watershed. This was done using the Zonal Statistics tool, which calculates raster statistics within the zones of a given polygon file. Then, by reclassifying the new Zonal Statistics layer into four classes, once again using Natural Breaks, a final map was generated that showed the flood

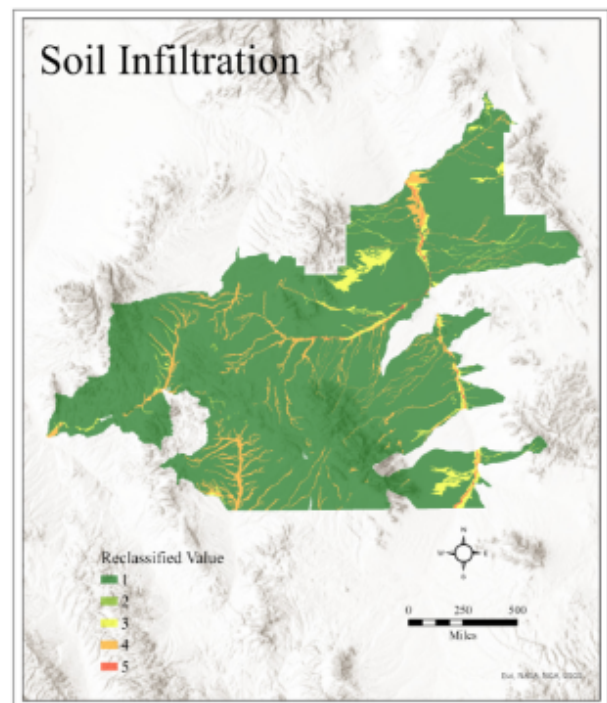


(a)

(b)



(c)

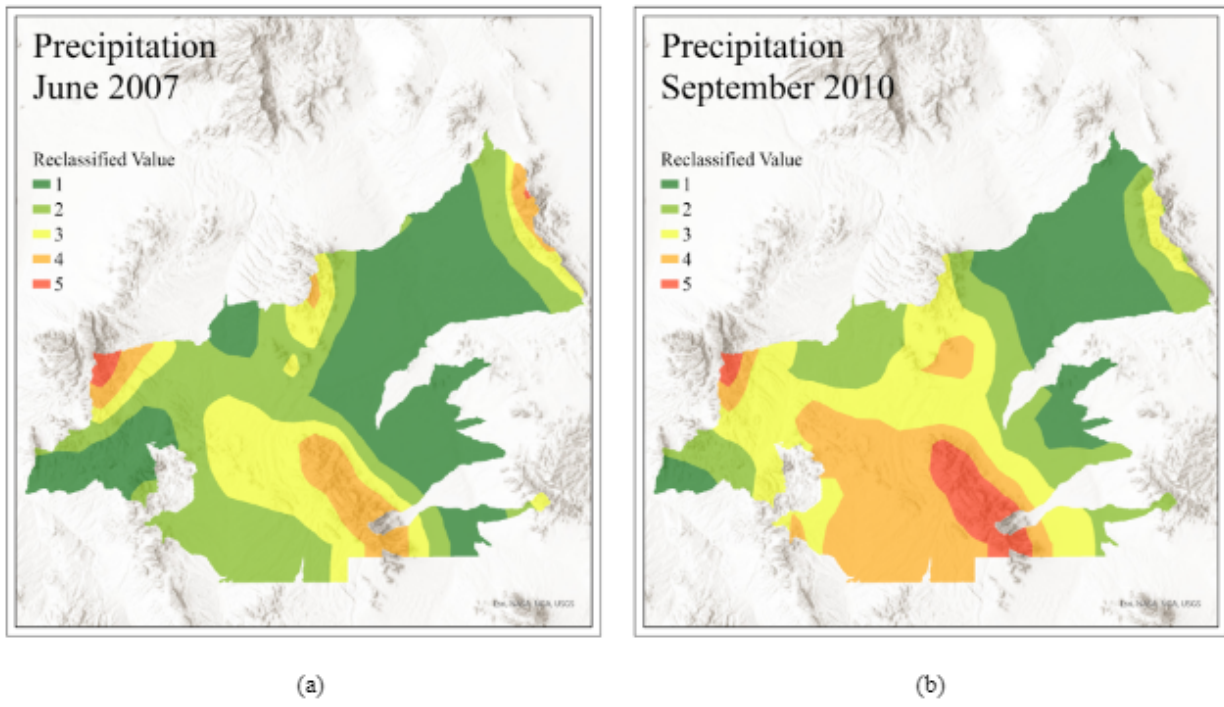


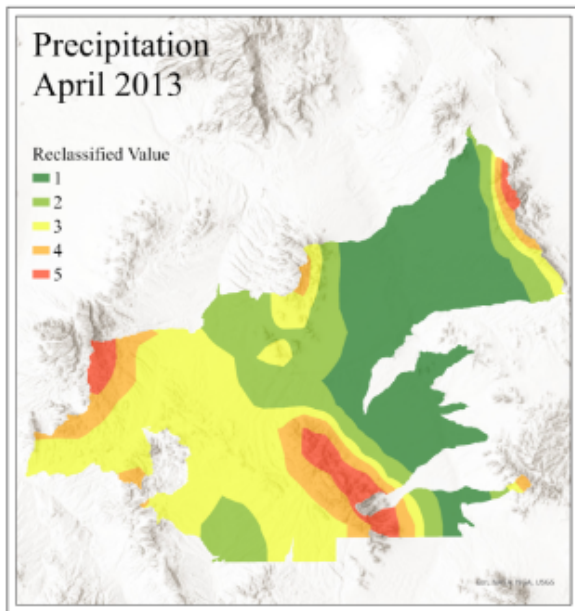
(d)

Figure 7: Maps showing the topographic variables once they were reclassified into values of 1 through 5: (a) Elevation, (b) Slope, (c) Distance to Nearest Streambed, (d) Soil Infiltration. Elevation, slope, and stream layers were reclassified using Natural Breaks. Since the dominant flood condition used in the soil infiltration layer is a categorical variable, the five flood conditions were reclassified as follows: ‘Never’ - 1, ‘Very Rare’ - 2, ‘Rare’ - 3, ‘Occasional’ - 4, ‘Frequent’ - 5.

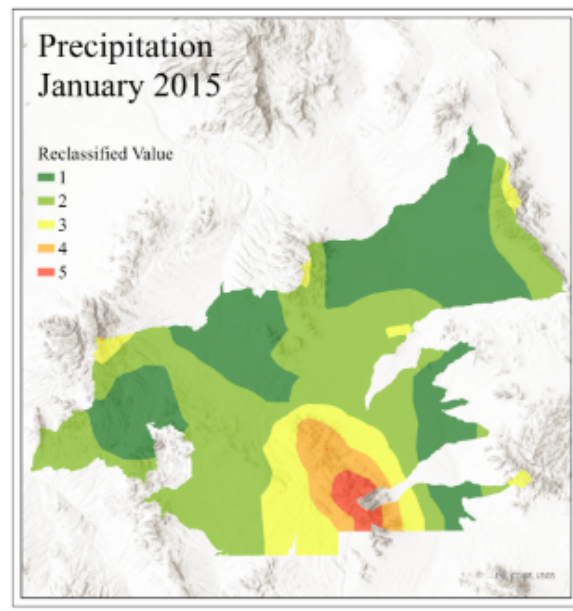
susceptibility for each watershed in the study area. Watersheds were classified as having either Low, Moderate, High, or Very High susceptibility to flooding.

Using the new Flood Susceptibility maps, the total number of wet ponds within each susceptibility class were added up and the proportion of wet ponds to the total number of ponds in each susceptibility class was calculated.

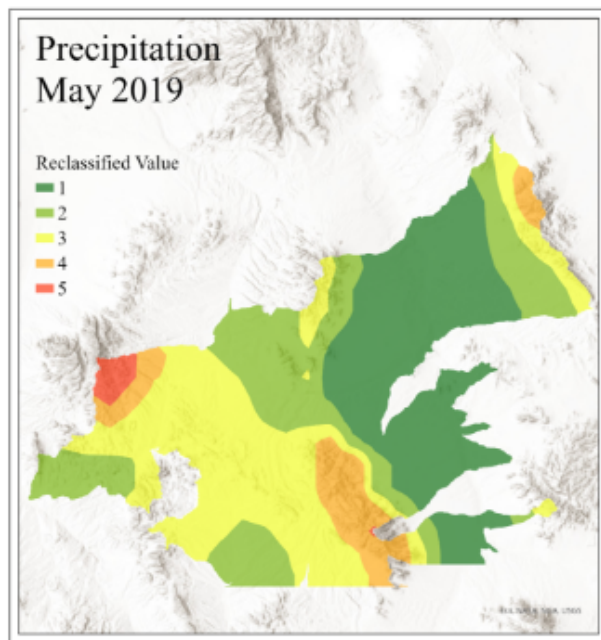




(c)



(d)



(e)

Figure 8: Maps showing rainfall layers for each study month after being reclassified into values of 1 through 5: (a) June 2007, (b) September 2010, (c) April 2013, (d) January 2015, (e) May 2019. Rainfall layers were classified using Natural Breaks.

3 Results and Discussion

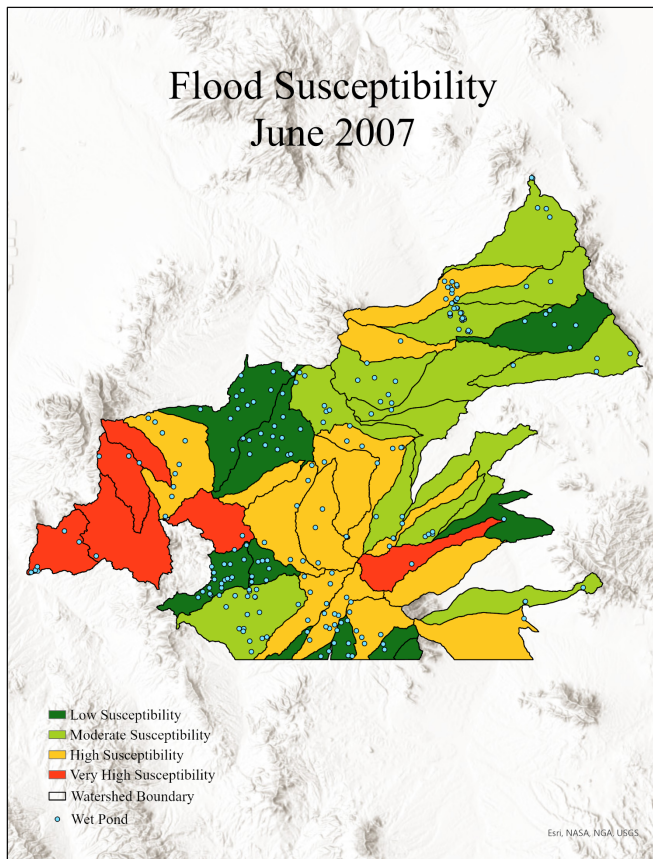
	June 2007			September 2010			April 2013			January 2015			May 2019			Avg. Prop.
	72	88	81.82 %	48	112	42.86 %	49	88	55.68 %	62	79	78.48 %	50	94	53.19 %	62.41%
Low Susceptibility	72	88	81.82 %	48	112	42.86 %	49	88	55.68 %	62	79	78.48 %	50	94	53.19 %	62.41%
Moderate Susceptibility	75	130	57.69 %	65	122	53.28 %	72	135	53.33 %	49	80	61.25 %	57	133	42.86 %	53.68%
High Susceptibility	64	94	68.09 %	57	84	67.86 %	62	120	51.67 %	98	163	60.12 %	45	99	45.45 %	58.64%
Very High Susceptibility	13	16	81.25 %	6	9	66.67 %	4	8	50.00 %	21	27	77.78 %	20	28	71.43 %	69.43%

Table 1

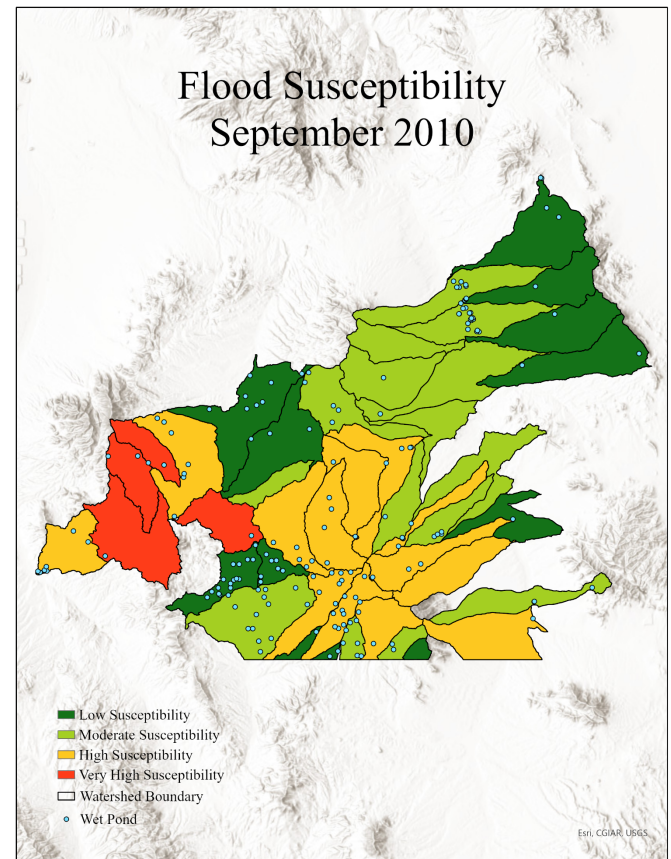
Table 1 shows the results of comparing wet ponds with different classes of flood susceptibility. Within each study month, there are three columns that represent, from left to right: total number of wet ponds located in watersheds with the given class of flood susceptibility, total number of ponds (wet or dry) located in watersheds with the given class of flood susceptibility, and the percentage of the total ponds located in each flood susceptibility class that were wet. For example, for May 2019, there were 20 wet ponds located in watersheds with ‘Very High Susceptibility’ and 28 wet or dry ponds in the same watersheds, meaning wet ponds accounted for 71.43% of all ponds in these watersheds. The column on the very right of the table shows the average proportion of wet ponds for each susceptibility class across all study months.

Table 1 shows that the correlation between flood susceptibility and inundated ponds varies across the study years. For June 2007, watersheds with Low Susceptibility and Very High Susceptibility had the highest proportion of wet ponds, with both classes having over 80% of their ponds inundated. For September 2010, watersheds with High Susceptibility and Very High Susceptibility both had more than 60% of their ponds inundated, which was a larger proportion than the other two classes. April 2013 only had slight differences in proportion of wet ponds across all four susceptibility classes, with watersheds in each class having between 50% and 55%

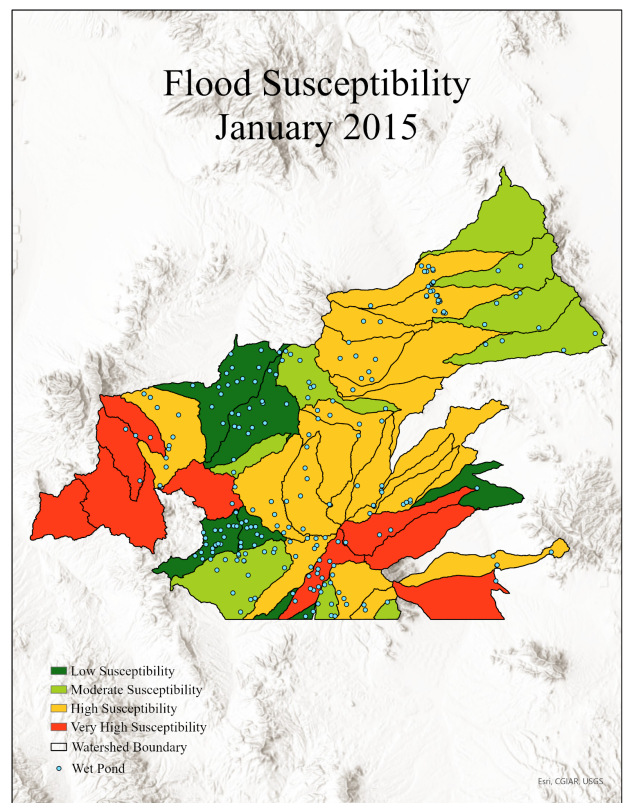
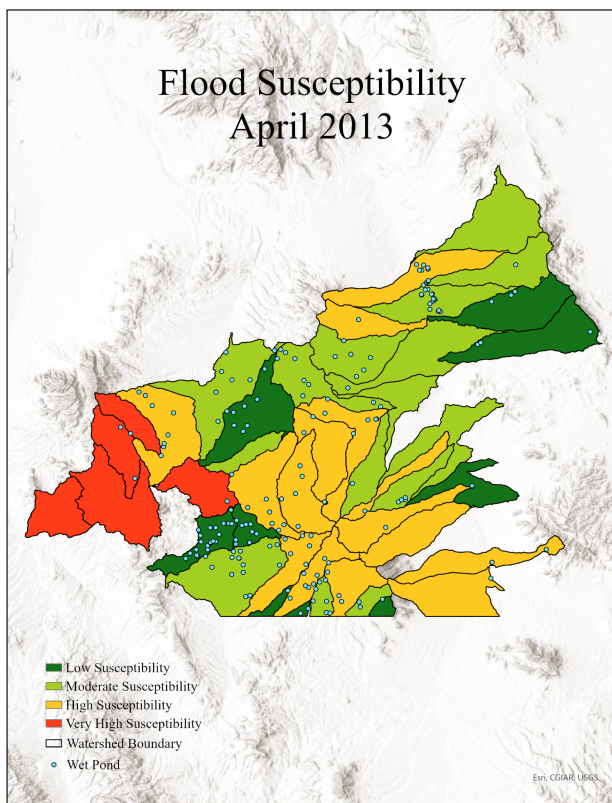
of their ponds inundated. January 2015 had the highest proportion of wet ponds located in watersheds with Low Susceptibility or Very High Susceptibility. Both classes had at least 77% of ponds with water in them. The watersheds with Very High Susceptibility in May 2019 had a significantly larger proportion of wet ponds when compared with the rest of the susceptibility classes, specifically 71.43%, which was more than 18% higher than the class with the second highest proportion of wet ponds. In terms of the average proportion of wet ponds for all five study months, Very High Susceptibility watersheds had the highest proportion, followed by Low Susceptibility, High Susceptibility, and Moderate Susceptibility watersheds, in that order.



(a)

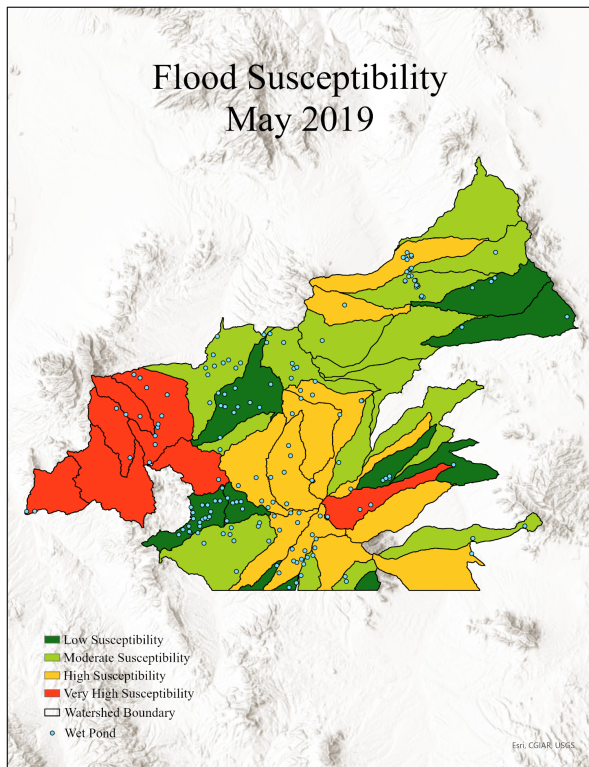


(b)



(c)

(d)



(e)

Figure 9: Maps showing the flood susceptibility for each watershed in the study region for each of the study dates: (a) June 2007, (b) September 2010, (c) April 2013, (d) January 2015, and (e) May 2019. Dark green and light green areas represent watersheds with low and moderate susceptibility to flooding, respectively. Yellow areas represent watersheds with high flood susceptibility and red areas represent the watershed with the highest susceptibility to flooding. Locations of inundated ponds for the given study month are represented with blue points.

3.1 Potential Improvements to this Study

Despite the fact that watersheds with very high flood susceptibility had the highest average proportion of wet ponds in this study, there are a few potential issues involved in the methods of this study that are worth addressing.

The first issue involves the soil data used in this model. More than 90% of the study area has a soil type with the dominant flood condition of ‘Never.’ Considering that soil was also weighted the least out of any variable in this study, the combination of these two factors might have made the soils layer somewhat redundant with regards to the model. When using this model in the future, it would be worth experimenting with an aspect of the soil that has more variation across the study area.

Another issue resides with the slope and elevation variables. Since steeper slopes are often found in higher elevations and vice versa, in locations containing extremes of either slope or elevation, the two variables are likely conflicting with one another in terms of the influence they have on flood susceptibility in that area. For example, the areas with the lowest elevations are relatively flat, meaning the degree of slope is very small. Areas like this would be highly susceptible to flooding in terms of elevation, but not very susceptible at all in terms of slope. Essentially, in areas of either extremely steep slope or the lowest elevations, the significant

influence that one of the variables should have on the flood susceptibility in that area is being reduced by the opposite variable's lack of influence. Future studies involving this model might benefit from reconsidering how these variables are used in the study, specifically elevation. Since the ecological effects of flooding are more significant at higher elevations, it would be worth testing if the effects of flooding on pond inundation at higher elevations are more significant than what was assumed in this study.

Despite the encouraging results that this study provided with regards to the proportion of wet ponds in watersheds of high flood susceptibility, some of the previous flood studies that were used to determine the weighting of variables for this study were conducted in areas that do not reflect the same climate as the region used in this study. While Iran is a semi arid environment similar to the southwestern United States (Choubin et al., 2018; Khosravi et al., 2018), the mountainous topography of both Vietnam and Romania create differences in precipitation volume compared to southeastern Arizona (Bui et al., 2019; Costache et al., 2019). Basing variable weights of off studies conducted in areas similar to the study area being used with this model would be more appropriate.

Although it is not weighted heavily in this study, better rainfall data would likely improve the accuracy of flood susceptibility modeling across the region. Since rain events in the area have both high spatial and temporal variability, the layers representing rainfall totals across the entire study area likely contained generalized rainfall totals that aren't completely consistent with the precipitation that happens in the region. While the results of this particular study were encouraging, applying the model to an area that has a more predictable and consistent precipitation cycle could be more useful compared to applying it to a monsoon environment.

4 Conclusion

The flood susceptibility model used in this study showed that watersheds within the study area that were found to be very highly susceptible to flooding had, on average, a larger proportion of inundated ponds compared to watersheds that were classified as having either low, moderate, or high susceptibility to flooding. Despite the encouraging results that this study provided relating to flood susceptibility and pond inundation in southeastern Arizona, addressing a few potential issues with the model would likely be beneficial in future uses of this model. Issues relating to soil classification, the relationship between slope and elevation, previous studies used as sources for data variable weights, and precipitation data are all aspects of this study that could be addressed in order to improve the efficacy and integrity of the model.

References

- Adams, D. K., & Comrie, A. C. (1997). The North American Monsoon, *Bulletin of the American Meteorological Society*, 78(10), 2197-2214. Retrieved Nov 16, 2022, from [https://doi.org/10.1175/1520-0477\(1997\)078%3C2197:TNAM%3E2.0.CO;2](https://doi.org/10.1175/1520-0477(1997)078%3C2197:TNAM%3E2.0.CO;2)
- Basri H, Syakur S, Azmeri A, Fatimah E. (2022) Floods and their Problems: Land uses and soil types perspectives *IOP Conf. Ser.: Earth Environ. Sci.* 951 012111. Retrieved Nov 23, 2022 from <https://doi.org/10.1088/1755-1315/951/1/012111>
- Bui D T, Tsangaratos P, Ngo P T, Pham T D and Pham B T (2019) Flash flood susceptibility modeling using an optimized fuzzy rule based feature selection technique and tree based ensemble methods *Sci. Total Environ.* 668 1038–54. Retrieved Nov 23, 2022 from <https://doi.org/10.1016/j.scitotenv.2019.02.422>

Choubin B, Moradi E, Golshan M, Adamowski J, Sajedi-Hosseini F, Mosavi A. (2018). An ensemble prediction of flood susceptibility using multivariate discriminant analysis, classification and regression trees, and support vector machines. *Sci. Total Environ.* 651 2087-2096. Retrieved Nov 24, 2022 from <https://doi.org/10.1016/j.scitotenv.2018.10.064>

Costache R, Pham QB, Sharifi E, Linh NTT, Abba SI, Vojtek M, Vojteková J, Nhi PTT, Khoi DN. (2019). Flash-Flood Susceptibility Assessment Using Multi-Criteria Decision Making and Machine Learning Supported by Remote Sensing and GIS Techniques. *Remote Sensing*. 2020; 12(1):106. Retrieved Nov 24, 2022 from <https://doi.org/10.3390/rs12010106>

Esri Inc. (2021). *ArcGIS Pro* (Version 2.9.0). Esri Inc.

<https://www.esri.com/en-us/arcgis/products/arcgis-pro/overview>

Esri Inc. (2019). USA Soils Map Units (SSURGO). Esri Inc. Retrieved Dec 6, 2022 from <https://www.arcgis.com/home/item.html?id=06e5fd61bdb6453fb16534c676e1c9b9>

Gendreau, K. L., Buxton, V. L., Moore, C. E., & Mims, M. C. (2021). Temperature loggers capture intraregional variation of inundation timing for intermittent ponds. *Water Resources Research*, 57, e2021WR029958. Retrieved Nov 16, 2022, from <https://doi.org/10.1029/2021WR029958>

Goodrich, D. C., Unkrich, C. L., Keefer, T. O., Nichols, M. H., Stone, J. J., Levick, L. R., and Scott, R. L. (2008), Event to multidecadal persistence in rainfall and runoff in southeast Arizona, *Water Resour. Res.*, 44, W05S14, Retrieved Nov 16, 2022, from doi:10.1029/2007WR006222.

Khosravi K, Pham B T, Chapi K, Shirzadi A, Shahabi H, Revhaug I, Prakash I, Tien Bui D, Shahabi H, Chapi K, Shirzadi A, Pham B T, Khosravi K and Revhaug I. (2018) A

comparative assessment of decision trees algorithms for flash flood susceptibility modeling at Haraz watershed, northern Iran *Sci. Total Environ.* 627 744–55. Retrieved Nov 23, 2022 from <https://doi.org/10.1016/j.scitotenv.2018.01.266>

Murray-Hudson, M., Wolski, P., Murray-Hudson, F. *et al.* Disaggregating Hydroperiod: Components of the Seasonal Flood Pulse as Drivers of Plant Species Distribution in Floodplains of a Tropical Wetland. *Wetlands* 34, 927–942 (2014). Retrieved Nov 27, 2022 from <https://doi.org/10.1007/s13157-014-0554-x>

Nhiwatiwa, T., Dalu, T. (2016). Seasonal variation in pans in relation to limno-chemistry, size, hydroperiod, and river connectivity in a semi-arid subtropical region, *Physics and Chemistry of the Earth, Parts A/B/C*, Volume 97, 2017, Pages 37-45, ISSN 1474-7065, Retrieved Dec 5, 2022 from <https://doi.org/10.1016/j.pce.2016.11.003>

Paton, P. W. C., & Crouch, W. B., III (2002). Using the phenology of pond-breeding amphibians to develop conservation strategies. *Conservation Biology*, 16(1), 194–204. Retrieved Dec 5, 2022 from <https://doi.org/10.1046/j.1523-1739.2002.00260.x>

PRISM Climate Group, Oregon State University [PRISM]. (2014). Retrieved Dec 6, 2022 from <https://prism.oregonstate.edu/>

Talbot, C.J., Bennett, E.M., Cassell, K. *et al.* The impact of flooding on aquatic ecosystem services. *Biogeochemistry* 141, 439–461 (2018). Retrieved Dec 5, 2022 from <https://doi.org/10.1007/s10533-018-0449-7>

U.S. Geological Survey [USGS]. 2022. U.S. Department of Agriculture - Natural Resources Conservation Service. Geospatial Data Gateway. Retrieved Dec 6, 2022 from <https://datagateway.nrcs.usda.gov/>

USGS and USDA - NRCS. 2022. Watershed Boundary Dataset (WBD). Retrieved Dec 6, 2022
from <https://gdg.sc.egov.usda.gov/Catalog/ProductDescription/WBD.html>